# *Experimental study and chemical affinity model on the inhibition of CO2 gas hydrate formation*

Chemical Engineering Science 281 (2023) 119158

Contents lists available at ScienceDirect

Chemical Engineering Science

journal homepage: www.elsevier.com/locate/ces

# Experimental study and chemical affinity model on the inhibition of $CO_2$ gas hydrate formation

Yongchao Rao [a,b], Shuli Wang [c,*], Yan Yang [a,e,*], Ru Jia [d], Shidong Zhou [a,b], Shuhua Zhao [a,b], Chuang Wen [e,f,*]

[a] School of Petroleum and Nature Gas Engineering, Changzhou University, Changzhou 213164, China
[b] Jiangsu Key Laboratory of Oil-Gas Storage and Transportation Technology, Changzhou University, Changzhou 213164, China
[c] School of Energy, Quanzhou Vocational and Technical University, Quanzhou, Fujian 362268, China
[d] Pipeline Storage and Transportation Company, Sinopec, Xuzhou 221008, China
[e] Faculty of Environment, Science and Economy, University of Exeter, Exeter EX4 4QF, UK
[f] School of the Built Environment, University of Reading, Reading RG6 6AH, UK

ARTICLE INFO

*Keywords:*
$CO_2$ gas hydrate
Hydrate formation
Affinity model
Compound inhibitor
Inhibition

ABSTRACT

Natural gas and water can form complex cage crystals in oil and gas pipelines under certain conditions. The natural gas hydrate formed after crystal clustering can block the pipeline and affect the operation efficiency of the pipeline, and even cause equipment damage, bringing economic and security problems to enterprises. In the present study, we experimentally investigated the inhibition of $CO_2$ formation hydrate using attapulgite (ATP) and glucose (GLC). The kinetic influence on the formation of $CO_2$ hydrate by the complex pairing of kinetic inhibitor ATP is conducted under the working conditions of 277.15 K and 3.5 MPa. The effect of compound inhibitors on the temperature and pressure conditions, growth process and gas consumption of hydrate formation are revealed. The chemical affinity model of $CO_2$ hydrate formation under a compound inhibitor system is derived and established based on experimental studies. The results show that the combination of GLC and ATP can inhibit the formation of $CO_2$ hydrate to varying degrees, prolong the induction time of hydrate, and reduce the consumption of $CO_2$. The optimized experimental studies demonstrate that the best inhibitory compound system is 15 mg/mL GLC + 1.00 mg/mL ATP. Compared with the pure water system and single 15 mg/mL GLC system, the induction time is extended by 122.61% and 122.23%, while the gas consumption is reduced by 23.72% and 3.41%. The results provide new ideas and methods for the prediction of hydrate formation in the compound inhibitor system for the safe operation of oil and gas pipelines.

## 1. Introduction

Natural gas and water can form complex cage crystals in oil and gas pipelines under certain conditions. The natural gas hydrate formed after crystal clustering will block the pipeline and affect the operation efficiency of the pipeline, and even cause equipment damage, bringing economic and security problems to enterprises (Sanatgar and Peyvandi, 2019; Chaturvedi et al., 2021; Abu Hassan et al., 2021). Hydrate risk control technology mainly uses low-dose hydrate inhibitors with the advantages of high efficiency and low dosage. Low-dose hydrate inhibitors are mainly composed of kinetic hydrate inhibitors and polymerization inhibitors, which have been extensively studied by relevant scholars. In terms of kinetic inhibitors, Kelland et al. (Kelland, 2006) tested a series of cyclic kinetic inhibitors and discussed their mechanisms. Srorr et al. (Storr et al., 2004) found a new type of amphoteric ion tri-butylpropyl ammonium sulfonate(TBAPS) inhibited the formation of hydrate. Ajiro et al. (Ajiro et al., 2014) synthesized a batch of polyamides with different branched chains and studied their inhibitory effects on the formation of tetrahydrofuran (THF) hydrate. Combined with the experimental results, the branched-chain structure and chain length with the best inhibitory effect were found. Villano et al. (Villano and Kelland, 2009) tested the effect of a series of hyperbranched polyether amine in THF and obtained the best size and dosage as a kinetic inhibitor. In addition, it is also concluded that the inhibition mechanism of kinetic inhibitors is not only adsorption. In the aspect of anti-polymerization agents, Huo et al. (Huo et al., 2001) tested many

* Corresponding authors.
*E-mail addresses:* wsl@cczu.edu.cn (S. Wang), y.yang7@exeter.ac.uk (Y. Yang), c.wen@reading.ac.uk (C. Wen).

https://doi.org/10.1016/j.ces.2023.119158
Received 21 April 2023; Received in revised form 2 August 2023; Accepted 3 August 2023
Available online 5 August 2023

different surfactants as anti-polymerization agents and proposed the use of anti-polymerization agents to evenly disperse hydrate particles in the oil phase system, so that it flows through the slurry form in the pipeline, and greatly reduces the possibility of pipeline blockage. Mehta et al. (Mehta and Sloan, 1994) proposed that the oil–water system becomes an emulsion after adding anti-polymerization agents, which can prevent further hydrate formation (Maryam and Pakizeh, 2017; Liu et al., 2013; Parisa et al., 2014). Kelland et al. (Kelland et al., 2006) proposed that some alkylamide surfactants can also be used as anti-polymerization agents. Peng et al. (Peng et al., 2008) suggested that the use of surfactants alone was not effective in preventing hydrate aggregation. Through systematic research, the anti-polymerization effect of Span 20 mixed with esters was obvious, and a series of evaluations were carried out in the circulating pipeline device. In addition, through many experiments, York et al. (York and Firoozabadi, 2008) found that when the main anti-polymerization agent failed, some small molecular alcohol dosages as low as 0.5 wt%, the anti-polymerization effect is also good. Koh et al. (Koh et al., 2002) shows that quaternary ammonium bromide has good hydrate growth inhibition, even if fewer kinetic inhibitors are used, it also makes up for many shortcomings of thermodynamic inhibitors. With the increasing use of kinetic inhibitors and the gradual emphasis on ecology, the environmental protection of kinetic inhibitors has attracted much attention. Therefore, many scholars began to pay attention to natural kinetic inhibitors. Lee et al. (Ju et al., 2007) studied the kinetic inhibitory effect of several cationic starches on the formation of methane, methane/ethane and methane/propane mixed gas hydrates and found that cassava starch increased the induction time (delayed crystallization) by an order of magnitude. It was also found that the addition of polyethylene oxide (PEO) in cassava starch could improve the properties of cassava starch and other starches and inhibit the memory effect of hydrate. Talaghat (Talaghat and Reza, 2014) used a small loop device to study starch, PEO and poly (propylene oxide) (PPO) for complex experiments. The results showed that the complex system showed a good synergistic effect, and PPO had a better synergistic effect. Kinetic inhibitor antifreeze proteins (AFPs) (Ohno et al., 2012; Ohno et al., 2010) delayed the crystallization process and showed better hydrate growth inhibition than the benchmark commercial inhibitor PVP. Zeng et al. (Zeng et al., 2006)found an AFP from deep-sea organisms, which had a certain effect on the inhibition of hydrate formation. Compared with PVP that has been commercialized, AFPs can not only better inhibit the formation of hydrate, but also reduce the memory effect of hydrate to a certain extent. Cha et al. (Cha et al., 2013) discovered polymers based on the reaction of polyvinyl alcohol with aldehydes. Arco, Texaco and BP conducted field applications of kinetic inhibitors (Sloan, 2005; Zerpa et al., 2011). Texaco conducted field applications of PVP in U.S. oil and gas fields. The results showed that PVP inhibited hydrate formation due to cold degree limitation (Zhao et al., 2016). BP first conducted field tests on KHI mixture in The North Sea gas field and West Sole/Hyde, and the results showed that the mixture had a good application effect (Huo et al., 2001).

Based on the above-mentioned literature survey, many researchers have conducted a series of studies on the inhibition effect of hydrate, but the inhibition law of green compound inhibitors on hydrate is still not fully understood. In the present study, the formation characteristics of $CO_2$ hydrate in the attapulgite and glucose compound system were evaluated, and the effects of compound inhibitor concentration, temperature and pressure on the formation of $CO_2$ hydrate were discussed in detail. The variation of gas consumption during the formation and growth of $CO_2$ hydrate crystals with time under the compound inhibitor system was analysed. The chemical affinity model of gas hydrate inhibition in the compound system was established, which provided a new theory and method for hydrate formation prediction in the compound inhibitor system.

The novelty of this present study is, firstly, to propose and develop a chemical affinity model to predict $CO_2$ hydrate formation. For instance, based on previous studies, Wang et al. (Xi et al., 2018; Yu et al., 2018; Li et al., 2020; Rao et al., 2020) investigated the effect of attapulgite and compound system on hydrate formation inhibition and rheological properties. The experimental results showed that the rich micro-channel structure of attapulgite crystal could absorb a large amount of water and effectively inhibit the formation of hydrate, but the kinetic model was not given. Secondly, we studied the effect of attapulgite on $CO_2$ hydrate formation which was not widely reported in the literature. For example, most of the existing hydrate inhibitors and polymer inhibitors are adverse to the ecological environment, and cannot be reused with simple effect (Li et al., 2017; Yan et al., 2018; Wang et al., 2020). The proposed utilization of attapulgite in the present study is not harmful to the natural environment and can be widely used which improves the sustainable development of oil and gas industries as the attapulgite is green, non-toxic, and it has a unique molecular sieves-like layer structure. Thirdly, we developed new composite inhibitors and proposed a hydrate inhibition model combined with theory to meet the current requirements for cost, environment and transportation efficiency. This improved the understanding of $CO_2$ hydrate formation under various complex conditions in the process of oil and gas exploitation and pipeline transportation.

## 2. Experiment studies

### 2.1. Experimental apparatus and materials

The experimental device is shown in Fig. 1. $CO_2$ is injected into the reactor by using a cylinder and an air compressor. Pressure is 0–30 MPa, and temperature is 0–20 °C. The volume of the visualization kettle is 500 mL. The ethylene glycol and water with a ratio of 3:1 were put into a low-temperature constant temperature water tank to carry cold. Table 1 is the details of experimental supplies involved in generating experiments. Combined with the screening results, the concentration of 5, 10, and 15 mg/mL of GLC and the concentration of 0.00, 0.50, 0.75, 1.00, 1.25 and 1.50 mg/mL of ATP were compounded to find out the best inhibitory concentration of $CO_2$ hydrate formation process.

### 2.2. Experimental steps

(1) Preparation of solution: The corresponding mass of solute needed in the experiment was weighed by electronic balance, put into the beaker cleaned by ultrasonic wave, and added with pure water. The beaker was sealed with preservative film, and the pores were used for ultrasonic oscillation rod insertion. After ultrasonic shock is completed, the reagent is sealed and stored in accordance with the specification. (2) Vacuum pumping: There are still water vapour and air in the connecting pipe and kettle. To ensure the accuracy of the experiment, it is necessary to open the vacuum pump for vacuum pumping. (3) Experimental reagent injection: open the inlet valve and inject 170 mL reagent into the reactor, and then close the inlet valve. (4) Vacuum again: To extract the gas dissolved in the reagent, the vacuum pump will be opened again for vacuum treatment until the pressure in the kettle is shown in the table to be reduced to negative pressure and maintained stably. (5) Circulating refrigeration: Before the experiment, the circulating refrigeration equipment was opened, and the water bath temperature was adjusted to the working condition (4) °C) to keep the temperature in the table stable at the set value and prepare to start the intake. (6) Data acquisition and recording: Open the data acquisition instrument and select the detection channel, open the software for data acquisition and recording. (7) Intake: The valve and intake valve of the gas storage cylinder are slowly opened. The pressure in the cylinder is used to inject $CO_2$ gas and the intake process is slowed down by controlling the valve to prevent the pressure surge in the kettle from damaging equipment and experimental data. During the intake process, attention should be paid to the intake stop when the pressure is lower than 0.5 MPa. Observe the recorded temperature, when the temperature drops to the set value, slowly open the valve intake again. After the intake air is finished, quickly close the

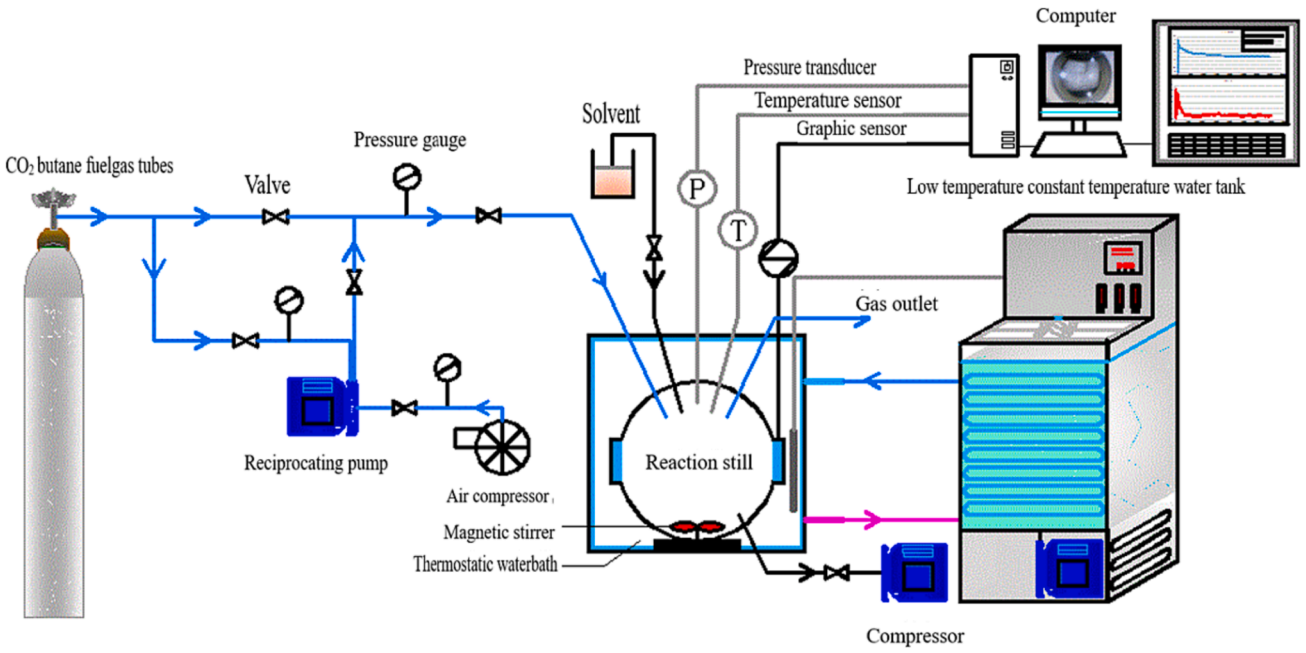


**Fig. 1.** Experimental figure for $CO_2$ hydrate formation.

**Table 1**
List of materials required for the experiments.

| Experimental materials | Molecular formula | Purity | Material source |
|---|---|---|---|
| Sucrose | $C_{12}H_{22}O_{11}$ | Analytical purity | Jiangsu Qiangsheng Functional Chemistry Co., Ltd |
| glucose | $C_6H_{12}O_6$ | Analytical purity | Jiangsu Qiangsheng Functional Chemistry Co., Ltd |
| Attapulgite soil | $Mg_5Si_8O_{20}(OH)_2(OH2)_4{\cdot}4H_2O$ | >99% | Anhui Mingmei Mineral Chemical Co., Ltd |
| carbon dioxide | $CO_2$ | >99% | Changzhou Jinghua Industrial Gas Co., Ltd |
| pure water | $H_2O$ | >99% | Laboratory Preparation |

valve in order. (8) Experiment: The stirrer was opened immediately after the intake air was finished, and the variation trend of temperature and pressure parameters and hydrate formation reaction was observed and recorded. The reaction in the kettle was observed by an optical fibre imaging system. The sign of hydrate formation is that the pressure in the kettle is stable and maintained for 30 min, and the reaction ends.

## 3. Chemical affinity model

Equations (1) and (2) are used to develop the chemical affinity model while we define $Q_i$ as reaction activity, such as formula (3).

$$A_i = -RT\ln\left(\xi_{Q_i}\right) \tag{1}$$

$$\xi_{Q_i} = \frac{Q_i}{K} \tag{2}$$

$$Q_i = \prod_j \left(\left(a_j\right)^{v_j}\right)_i \tag{3}$$

where $A_i^0 = RT\ln K$; $\xi_{Q_i}$ indicates the degree of reaction approaching equilibrium.

For a system with a closed fixed container and fixed temperature, the attenuation rate of affinity is expressed as:

$$A_{T,V} = \left(\frac{\partial A_i}{\partial t}\right)_{T,V} \tag{4}$$

$$A_{T,V} = A_r\left(\frac{1}{t}\right) + C_1 \tag{5}$$

$$C_1 = -A_r\left(\frac{1}{t_k}\right) \tag{6}$$

Insert (6) into (5) join (4) and we get (7):

$$A_{T,V} = A_r\left(\frac{1}{t} - \frac{1}{t_k}\right) \tag{7}$$

To correlate the chemical affinity parameters obtained from the experimental data with time, the time on both sides of Equation (7) is integrated to obtain:

$$\int_{t_i}^{t_k} A_i dt = A_r \int_{t_i}^{t_k} \left[\frac{1}{t} - \frac{1}{t_k}\right] dt \tag{8}$$

$$-A_i = A_r\left\{-\ln\left[\frac{t_i}{t_k}\exp\left(1 - \frac{t_i}{t_k}\right)\right]\right\} \tag{9}$$

Formula (9) Two sides are divided by*(-RT)*, then we can get:

$$\frac{A_i}{RT} = -\frac{A_r}{RT}\left[-\ln\left(\frac{t_i}{t_k}\exp\left(1 - \frac{t_i}{t_k}\right)\right)\right] \tag{10}$$

Define the reaction degree formula:

$$\zeta_{t_i} = \frac{t_i}{t_k} \tag{11}$$

During the formation of gas hydrate, the value of the driving force $A_i$ is related to gas consumption. Therefore, gas consumption in the process

of hydrate formation can be used to replace the active expression of the degree of the hydrate formation process. Formula (2) can be written into formula (12).

$$\zeta_{Q_i} = \frac{n_{ci}}{n_{cf}} = \frac{n_0 - n_i}{n_0 - n_f} \tag{12}$$

$$n_0 = \frac{P_0 V}{Z_0 RT}; n_f = \frac{P_f V}{Z_f RT} \tag{13}$$

From formula (12) and formula (13):

$$\zeta_{Q_i} = \frac{n_{ci}}{n_{cf}} = \frac{\frac{P_0}{Z_0} - \frac{P_i}{Z_i}}{\frac{P_0}{Z_0} - \frac{P_f}{Z_f}} \tag{14}$$

Combined formula (2) and formula (14), we get:

$$\frac{A_i}{RT} = -\ln\left(\frac{n_{ci}}{n_{cf}}\right) = -\ln\left(\frac{\frac{P_0}{Z_0} - \frac{P_i}{Z_i}}{\frac{P_0}{Z_0} - \frac{P_f}{Z_f}}\right) \tag{15}$$

Combined formula (10) and formula (15), we get:

$$\frac{n_{ci}}{n_{cf}} = \frac{\frac{P_0}{Z_0} - \frac{P_i}{Z_i}}{\frac{P_0}{Z_0} - \frac{P_f}{Z_f}} = \left[\frac{t_i}{t_k}\exp\left(1 - \frac{t_i}{t_k}\right)\right]^{\frac{-A_r}{RT}} \tag{16}$$

Taking logarithms on both sides of the Formula (16), we can obtain:

$$\ln\left(\frac{n_{ci}}{n_{cf}}\right) = \ln\left(\frac{\frac{P_0}{Z_0} - \frac{P_i}{Z_i}}{\frac{P_0}{Z_0} - \frac{P_f}{Z_f}}\right) = -\frac{A_r}{RT}\ln\left[\frac{t_i}{t_k}\exp\left(1 - \frac{t_i}{t_k}\right)\right] \tag{17}$$

Formula (17) can be changed into:

$$A_i = A_r \ln\left(\frac{t_i}{t_k}\exp\left(1 - \frac{t_i}{t_k}\right)\right) \tag{18}$$

Formula (18) is the same as formula (9) (Roosta et al., 2013; Karamoddin et al., 2014). Fig. 2 shows the flowchart to develop the chemical model for this study.

## 4. Experimental results and discussion

The effects of different concentrations of GLC and ATP on $CO_2$ hydrate formation temperature, pressure, $CO_2$ gas consumption and model parameters were investigated by combining experiments and simulations. Based on the comparison experiment and the model results, the inhibitory effect of the optimal compound concentrations of ATP, GLC and ATP + GLC on the formation of $CO_2$ hydrate was analysed.

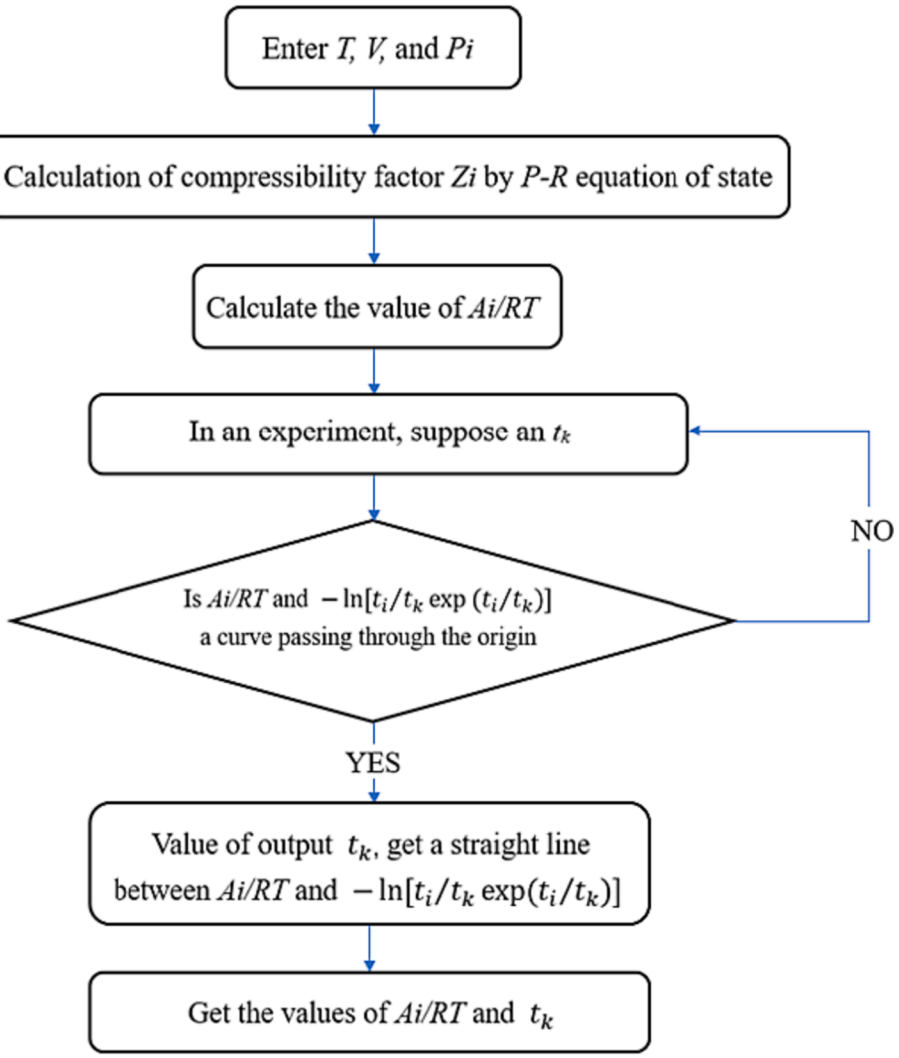


**Fig. 2.** Calculation logic diagram of kinetic parameters of chemical affinity model.

### 4.1. Effect of GLC and ATP combination on $CO_2$ hydrate formation process

The process of inhibiting $CO_2$ hydrate formation by the combination of GLC and ATP with different concentrations is roughly the same. Therefore, for the variation of the temperature and pressure process of hydrate formation under the composite inhibitor system, only a group of concentrations is selected for detailed analysis. Select 15 mg/mL GLC + 1.50 mg/mL ATP composite inhibitors, by analyzing the temperature and pressure changes in the process of hydrate formation, an in-depth understanding of the inhibitory effect of the composite inhibitor system on the $CO_2$ hydrate formation process. As shown in Fig. 3, under the initial conditions of 4 °C and 3.5 MPa, the hydrate formation process is roughly divided into four regions:

1) R1 region is the induction period before hydrate formation, and $CO_2$ rapidly dissolves in the composite solution. The initial pressure of 3.5 MPa in the reactor corresponds to 0 min on the time axis. Since $CO_2$ rapidly dissolves within 0–35 min, the pressure drops to 2.7 MPa. After 35 min, the pressure is almost constant, and the hydrate crystal nucleus begins to form in the reactor. The temperature corresponding to 0 min is higher than 4 °C in the experiment. The reason is that the temperature of $CO_2$ gas in the high-pressure reactor is higher than that set in the experiment. After entering the reactor from the gas cylinder, the temperature in the reactor also increases, but then the temperature in the reactor drops rapidly under the action of the constant temperature water bath device.

2) R2 region belongs to the rapid growth period. When the hydrate curve enters the R2 region from R1, the temperature and pressure change sharply, and the time is about 70 min. It is mainly due to the rapid action of $CO_2$ during the induction period to form a large number of hydrates and release a lot of heat, resulting in a sudden increase in the temperature curve of hydrates and a sudden decrease in the pressure curve. When the reaction time reached 224 min, the pressure decreased gradually.

3) R3 region belongs to the slow-growth region. Because the pressure decreases rapidly, the hydrate formation rate is reduced, and the $CO_2$ consumption and the heat generated by hydrate formation are also reduced.

4) R4 region belongs to the growth stop region. Temperature and pressure values from R3 to R4 after being roughly unchanged, can be identified in the region no longer hydrate growth, monitoring the kettle pressure value is about 2 MPa, the pressure curve has been stable, and can be determined that the pressure has remained unchanged.

Fig. 4 shows the reaction process of inhibiting the formation of $CO_2$ hydrate by the composite inhibitor system with the concentration of 15 mg/mL GLC + 1.50 mg/mL ATP captured by the high-speed camera in the reactor. The regions A, B, C and D in Fig. 4 and R1, R2, R3 and R4 in Fig. 4 were analysed, and the following conclusions were obtained. The hydrate in Fig. 4A had not yet formed, and $CO_2$ gas was fully dissolved in the solution before entering the induction period. Hydrate had not been observed in Fig. 4. ATP suspension solution made the kettle appear milky white, and the light transmittance was good and uniform, indicating that ATP in the kettle was uniformly dispersed and suspended well. In Fig. 4B, the hydrate is in the rapid growth stage. The hydrate first forms at the gas–liquid interface and a large number of hydrate particles gather and increase continuously. The transmittance in the kettle decreases with the formation of hydrate. At the same time, due to the role of the magnetic stirring device, the hydrate moves continuously and its structure is in a loose state. Fig. 4C is at the slow growth stage of hydrate. It can be seen that many hydrates have begun to gather into blocks, indicating that the hydrate formation reaction gradually reaches the equilibrium state, and the reaction rate also gradually slows down. Fig. 4D is at the end of the reaction state, temperature and pressure tend to be stable. And hydrate particles can still move with the stirrer, and the structure is still loose.

To more intuitively reflect the effect of GLC and ATP compound inhibitor systems on the inhibition performance of $CO_2$ hydrate formation, this study compared and analysed the temperature–pressure curve of $CO_2$ hydrate formation process from pure water and compound inhibitor system and drawn as Fig. 5. Under the same initial conditions (4 °C, 3.5 MPa), the diagram more intuitively reflects the concentration of 15 mg/mL GLC + 1.50 mg/mL ATP composite inhibitor system can inhibit the formation of $CO_2$ hydrate temperature and pressure changes over time.

In the temperature curve, $CO_2$ began to dissolve after intake, and the temperature in the kettle began to decrease because of the constant temperature water bath device. From the slope point of view, the temperature drop in the kettle under the compound inhibitor system is slower, and the time required to reach the experimental set temperature

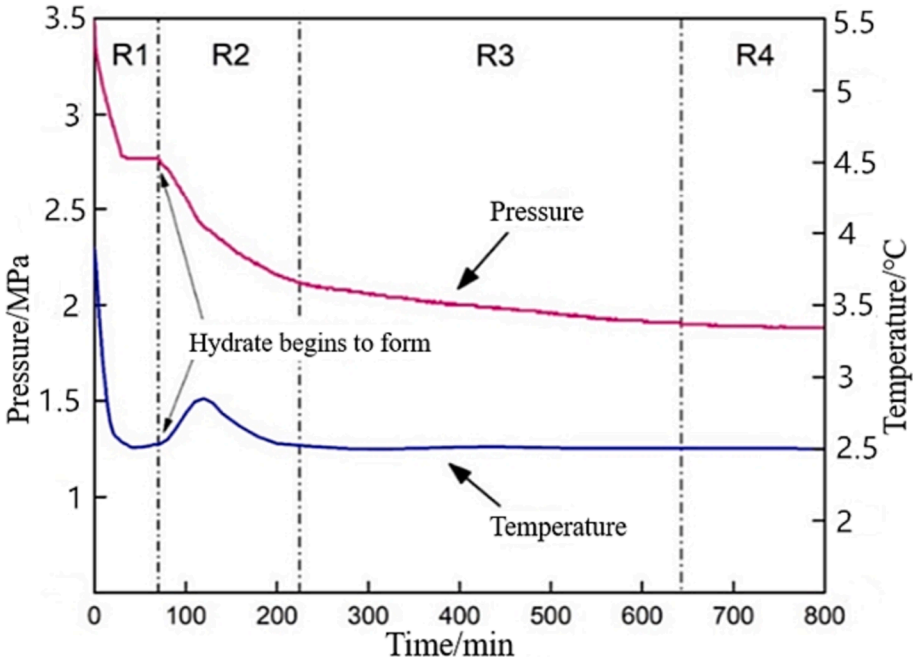


**Fig. 3.** GLC and ATP compound inhibitor system inhibits $CO_2$ hydrate formation temperature and pressure curve changes.

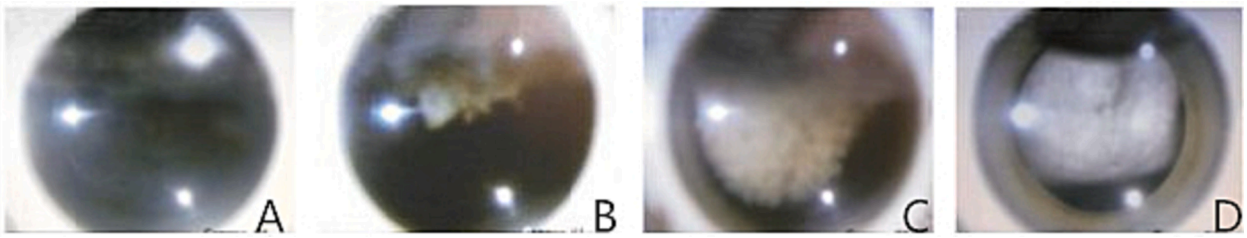


**Fig. 4.** Formation process of $CO_2$ hydrate in glucose and ATP complex system.

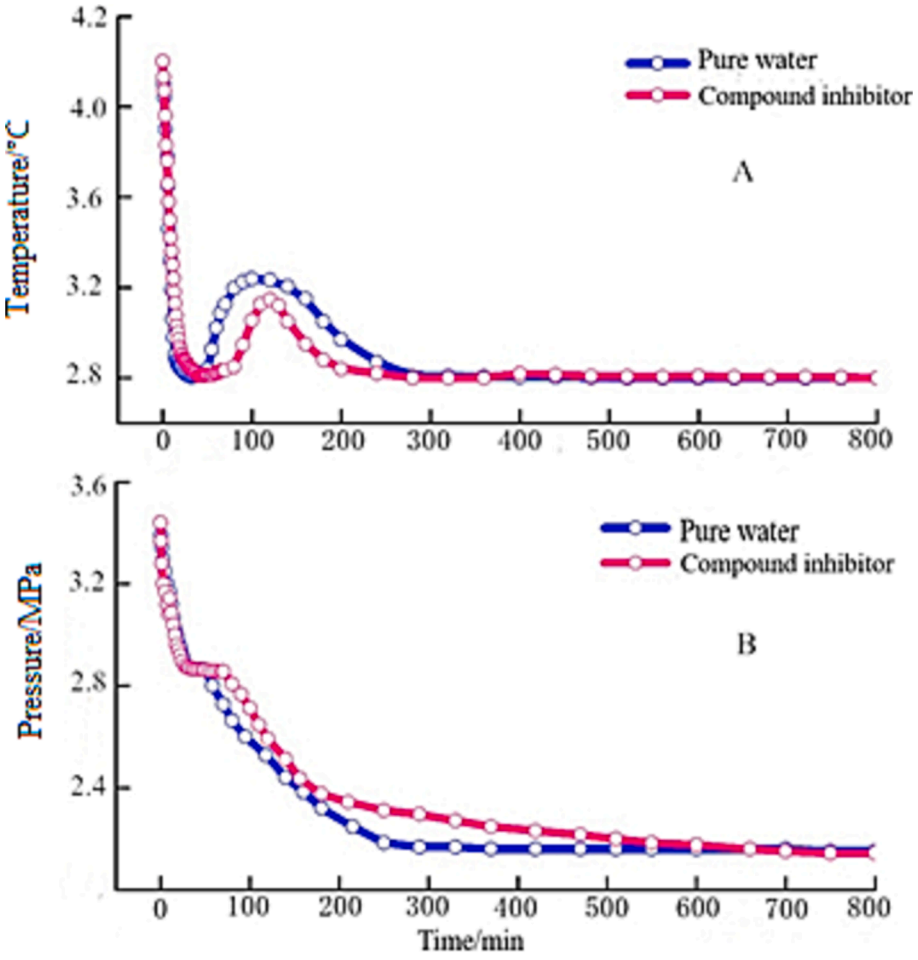


**Fig. 5.** Comparison of temperature and pressure curves of composite inhibitor system and distilled water system.

is longer than that of the pure water system. Due to the release of a large amount of heat to generate hydrate, the temperature curve rises sharply after the induction period. In the composite inhibitor system, the temperature in the kettle suddenly increased at about 70 min, while in the pure water system, the temperature suddenly increased at about 50 min, indicating that the composite inhibitor system increased the induction time of hydrate formation.

By observing the pressure curve, it was found that $CO_2$ gas in the two curves was dissolved in water 40 min ago, indicating that the presence of GLC and ATP in the system had no significant effect on the dissolution of $CO_2$. The pressure curve of 15 mg/mL GLC + 1.50 mg/mL ATP composite inhibitor system was significantly higher than that of the pure water system, and the composite inhibitor system also prolonged the formation time of $CO_2$ hydrate. At about 300 min, the growth phase of hydrate stopped in the pure water reaction, and the pressure at this time remained unchanged, while the growth phase of hydrate in the composite inhibitor system experienced two stages of rapid growth and slow growth. This indicated that the composite inhibitor system prolonged the induction time of hydrate formation, and the total growth time of hydrate was also prolonged by about 330 min, which was about 122.61% higher than that of the pure water system. The formation time of hydrate becomes longer according to the experimental result, which indicates that the inhibitor plays a role in the hydrate formation. The combined inhibitor inhibits the formation of hydrate, and it controls the amount of hydrate formation. The risk of pipeline blockage has been reduced, and it is conducive to the safe operation of oil and gas pipelines.

Fig. 6 shows the repeated experiments for five times. The initial conditions are 4 °C and 3.5 MPa, respectively. It can be seen that the pressure data of the five experimental systems are no significant difference among them although there is some tiny discrepancy with the time between 200 and 500 mins. The coincidence degree of the pressure change curve is quite good, which indicates that the experiment has

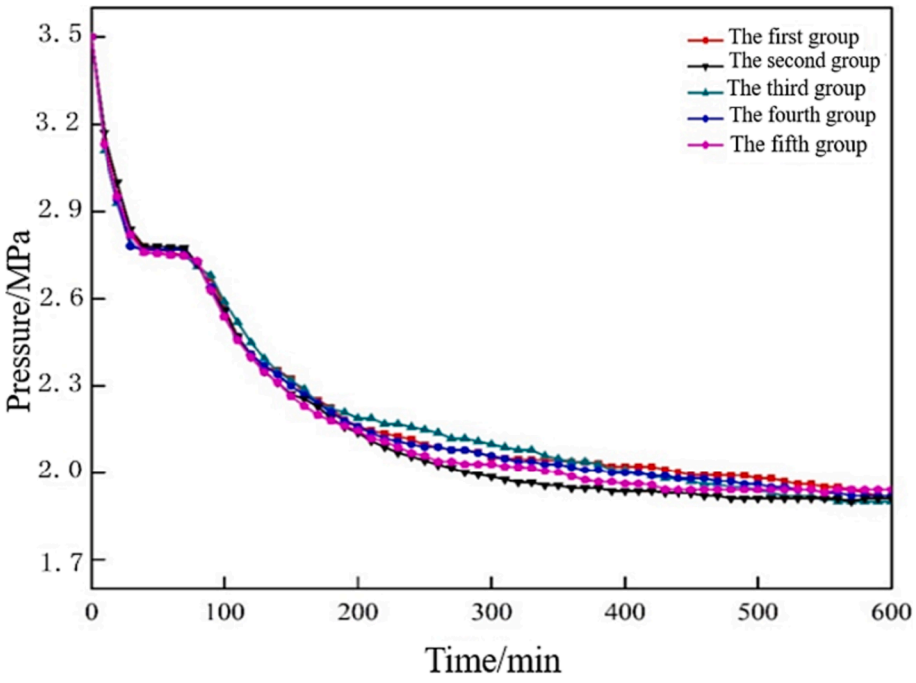


**Fig. 6.** $CO_2$ hydrate of compound inhibitor system with 15 mg/mL glucose + 1.50 mg/mL ATP generate experimental repeatability verification chart.

excellent repeatability.

### *4.2. Effect of GLC and ATP combination on gas consumption of $CO_2$ hydrate formation*

The operating conditions shown in Figs. 7 to 9 are 4 °C, 3.5 MPa and 450 r/min. In the initial stage of the reaction, the consumption of $CO_2$ gas increased rapidly due to the rapid dissolution of $CO_2$ gas into the solution. As the hydrate formation reaction proceeds, the $CO_2$ gas consumption curve rises slowly due to its complete dissolution in water until it no longer rises. Hydrate crystals grow with the dissolution process. As the growth of hydrate clusters reaches the critical size, $CO_2$ consumption in the reactor suddenly increases during the rapid growth stage of hydrate.

The complex system of GLC and ATP reduces the consumption of $CO_2$ gas, which has a more obvious inhibitory effect on the formation of $CO_2$ hydrate than the single GLC system. Under the action of compound inhibitors, the gas consumption curve showed a significant decrease, and the consumption of $CO_2$ was also significantly reduced. 15 mg/mL GLC + 1.00 mg/mL ATP was the best compound concentration, and the gas consumption was 0.23 mol in 0–600 min. Compared with the pure water system and single 15 mg/mL GLC system, the gas consumption decreased by 23.72% and 3.41% respectively.

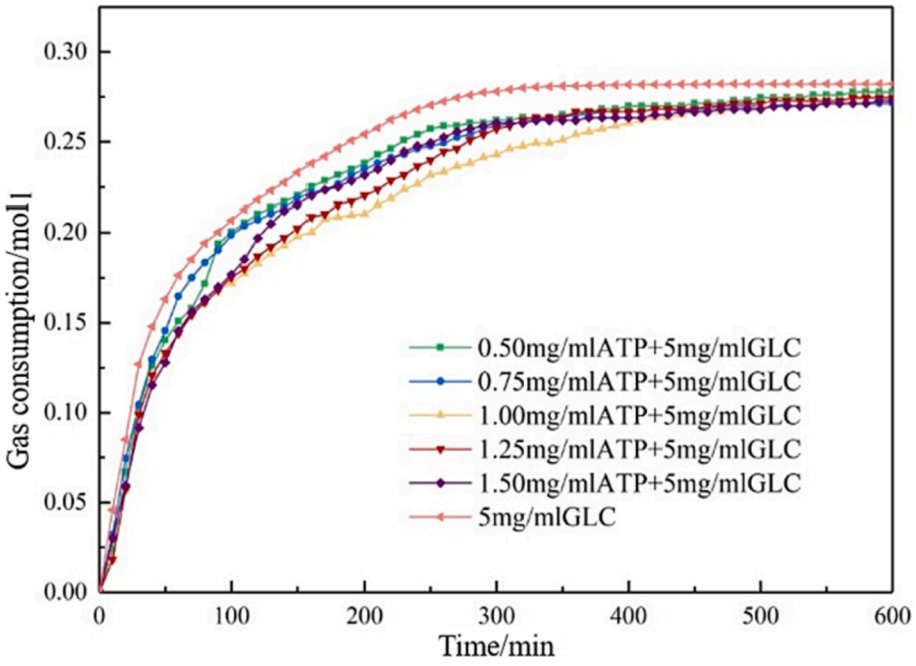


**Fig. 7.** Gas consumption curve in the process of inhibiting $CO_2$ hydrate formation by 5 mg/ml glucose combined with various concentrations of ATP.

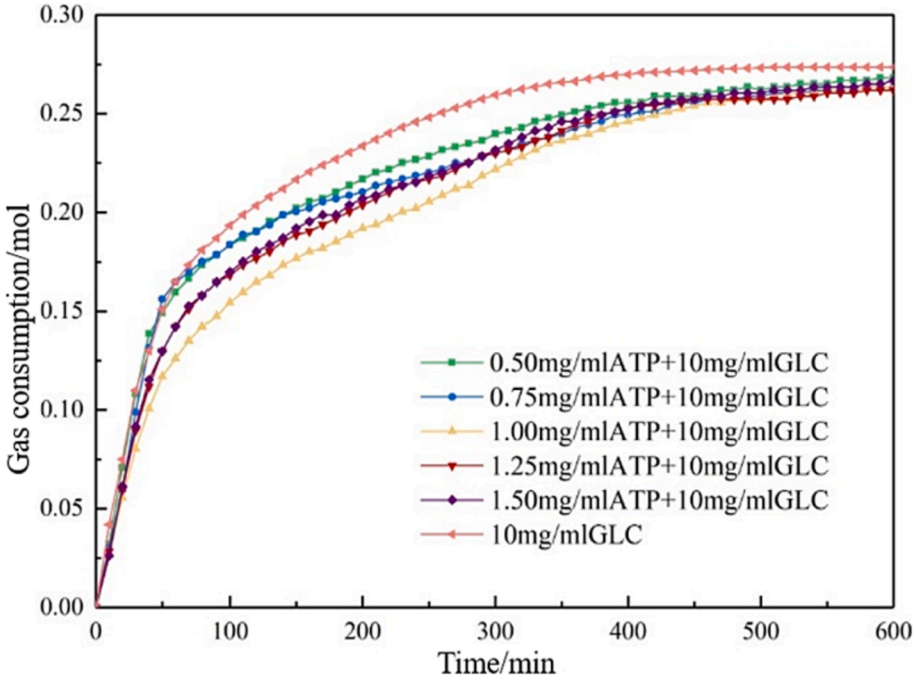


**Fig. 8.** Curve of gas consumption during $CO_2$ hydrate formation inhibited by 10 mg/ml glucose combined with various concentrations of ATP.

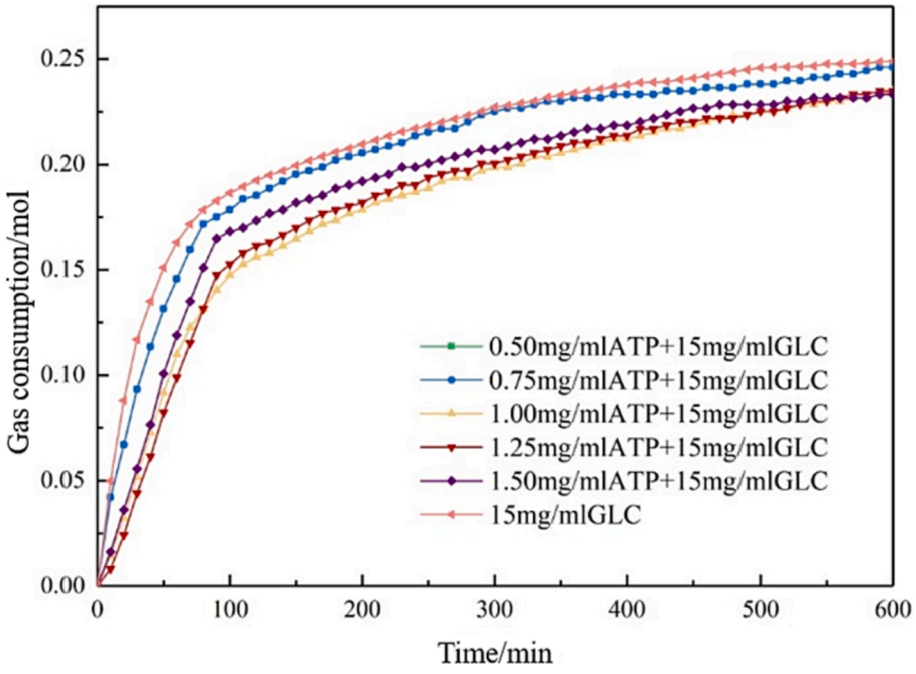


**Fig. 9.** Gas consumption curve in the process of inhibition of $CO_2$ hydrate formation by the mixture of 15 mg/ml glucose and various concentrations of ATP.

### *4.3. Effect of GLC and ATP combination on induction time of $CO_2$ hydrate formation*

The induction time was determined by the pressure change method, and the initial conditions were 3.5 MPa and 4 °C. It can be seen from Fig. 10 that compared with a single GLC inhibition system and a single ATP inhibition system, the induction time of hydrate formation in the GLC and ATP complex system was significantly prolonged, indicating that the presence of GLC in the GLC and ATP complex system enhanced the ability of ATP to inhibit hydrate formation. However, with the increase in ATP content, the induction time was gradually shortened. The reason may be that with the increase of ATP concentration, the micropore channels of ATP crystals were blocked due to mutual stacking, thus hindering the adsorption of water molecules by crystals during nucleation. It can be seen that the best concentration of compound inhibitor for prolonging the induction time is 15 mg/mL GLC + 1.00 mg/mL ATP. Compared with the single inhibitor system (15 mg/mL GLC), the induction time is prolonged by 122.23%.

## 5. Chemical affinity model analysis

The chemical affinity model was used to calculate and fit the

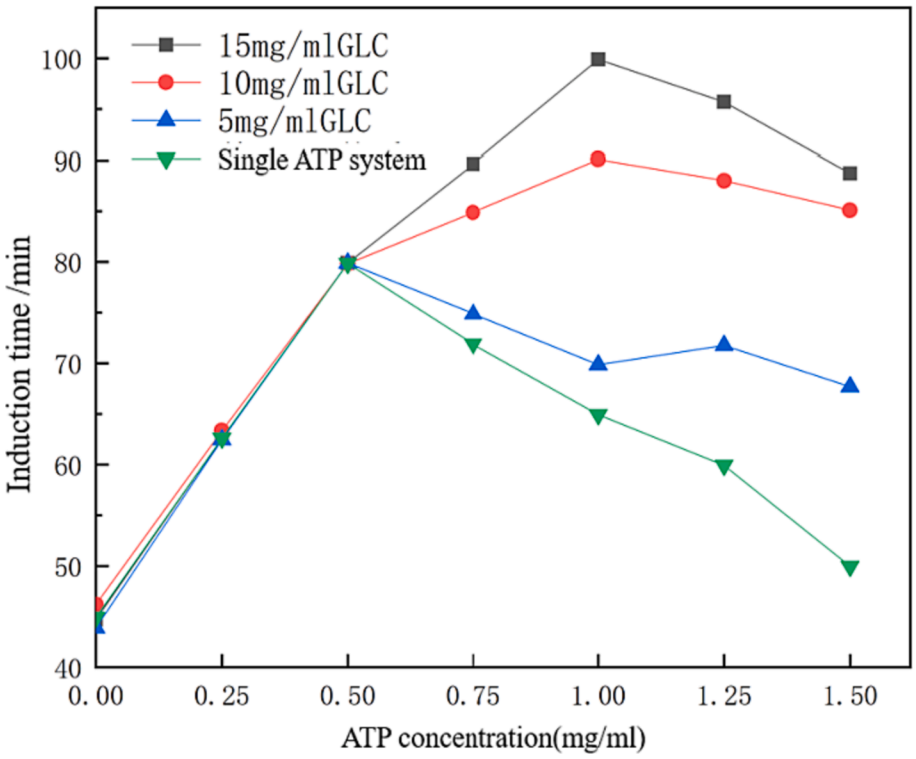


**Fig. 10.** Induction time of $CO_2$ hydrate formation in different systems.

experimental data, analyse the influence of the compound concentration of GLC and ATP, and verify the experimental conclusions from the model perspective. Under the experimental conditions of 4 °C, 3.5 MPa and 450 r/min, the fitting degree between the experimental results and the model results is verified by comparing the experimental data with the calculated parameters (pressure and gas consumption) of the model.

### 5.1. *Effect of inhibitor concentration on chemical affinity parameters*

Under the experimental conditions of 4 °C, 3.5 MPa and 450 r/min, the chemical affinity kinetic parameters of the GLC-ATP complex system at various concentrations show that the composite inhibitor system of GLC and ATP can delay the reaction of $CO_2$ hydrate to reach equilibrium, and the effect is more obvious under the composite inhibitor system of 15 mg/mL GLC + 1.0 mg/mL ATP. In the compound inhibitor system of this concentration, the inhibition effect is the best ($-A_r/RT$ = 0.2126). With the increase of the compound concentration of GLC and ATP, the equilibrium pressure increased first and then decreased as shown in Table 2.

### 5.2. *Model verification*

Figs. 11 and 12 are the composite inhibitor system of 15 mg/mL GLC + 1.00 mg/mL ATP under the experimental conditions of 4 °C, 3.5 MPa and 450 r/min. It shows that the experimental data are fitted with the chemical affinity model and the error is small, which can predict the formation of hydrate. The calculated $A_r/RT$ is almost a constant, so the same slope ($-A_r/RT$ = 0.233) can be used to study and predict the formation of $CO_2$ hydrate.

## 6. Conclusions

The compound system of GLC and ATP could prolong the induction time. Compared with the pure water system, the induction time increased significantly before the formation of nuclei in the system when GLC and ATP were mixed. Under the compound condition, GLC could significantly enhance the effect of ATP inhibitors on prolonging the induction time. In this study, 15 mg/mL GLC + 1.00 mg/mL ATP was the most significant experimental proportion to prolong the induction time. Compared with the pure water system and single 15 mg/mL GLC system, the induction time was prolonged by 122.61% and 122.23% respectively. The compound system of GLC and ATP can reduce $CO_2$ gas consumption, and the inhibitory effect is stronger than that of the system

**Table 2**
Effect of compound inhibitor system of glucose and ATP on chemical affinity parameters.

| Serial number | Concentration(mg/ml) | | Model parameter | | Pressure(MPa) | |
|---|---|---|---|---|---|---|
| | GLC | ATP | $t_k$(s) | $-Ar/RT$ | $P_0$ | $P_f$ |
| 1 | 0 | 0 | 11,567 | 0.2666 | 3.5 | 1.566698 |
| 2 | 0 | 0.5 | 36,385 | 0.2567 | 3.5 | 1.59968 |
| 3 | 0 | 0.75 | 36,337 | 0.2665 | 3.5 | 1.648915 |
| 4 | 0 | 1.0 | 36,315 | 0.2699 | 3.5 | 1.645968 |
| 5 | 0 | 1.25 | 36,190 | 0.2589 | 3.5 | 1.665965 |
| 6 | 0 | 1.5 | 35,088 | 0.255 | 3.5 | 1.62629 |
| 7 | 5 | 0 | 35,008 | 0.2829 | 3.5 | 1.618885 |
| 8 | 5 | 0.5 | 35,061 | 0.2715 | 3.5 | 1.621958 |
| 9 | 5 | 0.75 | 36,296 | 0.2571 | 3.5 | 1.62629 |
| 10 | 5 | 1.0 | 36,356 | 0.2574 | 3.5 | 1.607228 |
| 11 | 5 | 1.25 | 37,042 | 0.2561 | 3.5 | 1.602465 |
| 12 | 5 | 1.5 | 36,994 | 0.2306 | 3.5 | 1.866698 |
| 13 | 10 | 0 | 36,972 | 0.2505 | 3.5 | 1.748915 |
| 14 | 10 | 0.5 | 36,847 | 0.2429 | 3.5 | 1.759048 |
| 15 | 10 | 0.75 | 35,745 | 0.239 | 3.5 | 1.665965 |
| 16 | 10 | 1.0 | 35,657 | 0.2669 | 3.5 | 1.62629 |
| 17 | 10 | 1.25 | 35,718 | 0.2555 | 3.5 | 1.618885 |
| 18 | 10 | 1.5 | 35,948 | 0.2411 | 3.5 | 1.621958 |
| 19 | 15 | 0 | 36,953 | 0.2414 | 3.5 | 1.62629 |
| 20 | 15 | 0.5 | 37,013 | 0.2401 | 3.5 | 1.788915 |
| 21 | 15 | 0.75 | 38,565 | 0.2312 | 3.5 | 1.82146 |
| 22 | 15 | 1.0 | 38,975 | 0.2126 | 3.5 | 1.906698 |
| 23 | 15 | 1.25 | 38,765 | 0.2366 | 3.5 | 1.705965 |
| 24 | 15 | 1.5 | 37,879 | 0.2455 | 3.5 | 1.66629 |

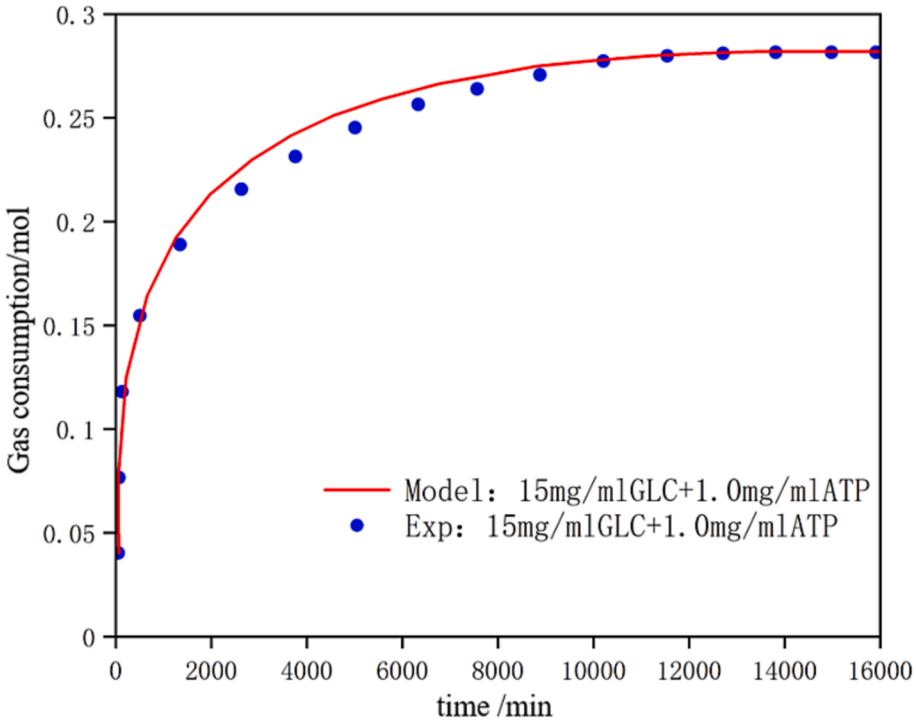


**Fig. 11.** Comparison of gas consumption calculated by experiment and model in the compound system of 15 mg/mL glucose + 1.00 mg/mL ATP.

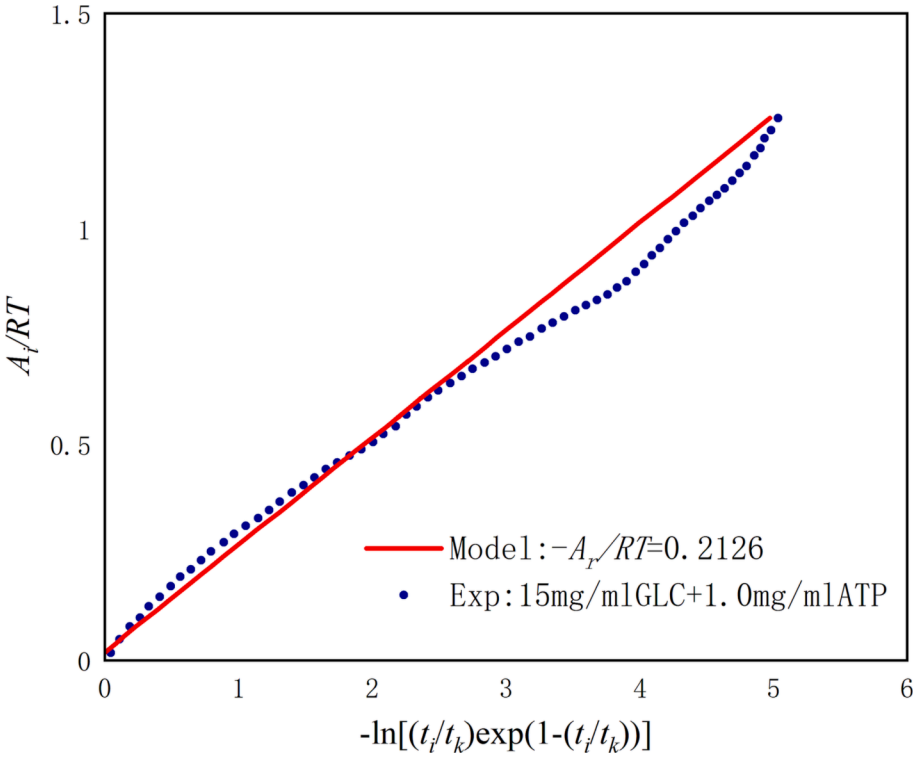


**Fig. 12.** Change curve of affinity with $-\ln[(t_i/t_k)\exp(1-(t_i/t_k))]$ during the formation of $CO_2$ hydrate in the complex system of 15 mg/mL glucose + 1.00 mg/mL ATP.

with only GLC. The best experimental system was 15 mg/mL GLC + 1.00 mg/mL ATP. Compared with pure water and a single 15 mg/mL GLC system, the gas consumption in 0 - 600 min was 0.23 mol, and the gas consumption decreased by 23.72% and 3.41%, respectively.

## Declaration of Competing Interest

The authors declare that they have no known competing financial interests or personal relationships that could have appeared to influence the work reported in this paper.

## Data availability

Data will be made available on request.

## Acknowledgements

This work was supported by the National Nature Science Foundation of China (No.51574045 & 51974037), the CNPC Innovation Foundation (No.2020D-5007-0211), the Project of Emission Peak and Carbon Neutrality of Jiangsu Province, China (No. BE2022001-5), the General Project of Natural Science Research in Jiangsu Universities (No.22KJB440002), Quanzhou Science and Technology Planning Project (No.2022 N045), the Vice General Project of Science and Technology of Jiangsu Province (No.FZ20211199), Open Project of Collaborative Innovation Center for Clean Energy Application Technology (Quanzhou Vocational and Technical University) (No. QJNY22-06), and the Opening Fund of Jiangsu Key Laboratory of Oil-gas Storage and Transportation Technology (Changzhou University) (No.CDYQCY202105).

## References

Abu Hassan, M.H., Sher, F., Sehar, S., Rasheed, T., 2021. Hydrothermally engineered enhanced hydrate formation for potential $CO_2$ capture applications. J. Environ. Chem. Eng. 9, 106515.

Ajiro, H., Takemoto, Y., Akashi, M., Chua, P.C., Kelland, M.A., 2014. Study of the kinetic hydrate inhibitor performance of a series of poly. Energy Fuels 24, 6400–6410.

Cha, M., Shin, K., Seo, Y., Shin, J.Y., Kang, S.P., 2013. Catastrophic growth of gas hydrates in the presence of kinetic hydrate inhibitors. Chem. A Eur. J. 117, 13988–13995.

Chaturvedi, K.R., Pandey, A., Kumar, R., Sharma, T., 2021. Role of hydrogen to promote hydrate formation of flue gas mixture of $CO_2$ and N-2 in silica nanofluid of single-step origin. J. Environ. Chem. Eng. 9, 106591.

Huo, Z., Freer, E., Lamar, M., 2001. Hydrate plug prevention by anti-agglomeration. Chem. Eng. Sci. 56, 4979–4991.

Huo, Z., Freer, E., Lamea, M., 2001. Investigation into THF hydrate slurry flow behaviour and inhibition by an anti-agglomerant. RSC Adv. 8, 122–125.

Ju, D.-L., Wu, H., Englezos, P., 2007. Cationic starches as gas hydrate kinetic inhibitors. Chem. Eng. Sci. 62, 6548–6555.

Karamoddin, M., Varminian, F., Daraee, M., 2014. Kinetic study on the process of $CHClF_2$ (R22) hydrate formation in the presence of SDS surfactant based on chemical affinity. J. Nat. Gas Sci. Eng. 19, 46–51.

Kelland, M.A., 2006. History of the development of low-dosage hydrate inhibitors. Energy Fuels 20, 825–847.

Kelland, M.A., Svartaas, T.M., Vsthus, J., Tomita, T., Mizuta, K., 2006. Studies on some alkylamide surfactant gas hydrate anti-agglomerants. Chem. Eng. Sci. 61, 4290–4298.

Koh, C.A., Westacott, R.E., Zhang, W., Hirachand, K., Soper, A.K., 2002. Mechanisms of gas hydrate formation and inhibition. Fluid. Phase. Equilibr. 194–197, 143–151.

Li, D.L., Peng, H., Liang, D.Q., 2017. Thermal conductivity enhancement of clathrate hydrate with nanoparticles. Int. J. Heat. Mass. Tran. 104, 566–573.

Li, L.J., Zhao, S.H., Wang, S.L., Rao, Y.C., 2020. $CO_2$ hydrate formation kinetics based on a chemical affinity model in the presence of GO and SDS. RSC Adv. 10, 12451–12459.

Liu, H., Mu, L., Wang, B., Liu, B., Wang, J., Zhang, X.X., Sun, C.Y., Chen, J., Jia, M.L., Chen, G.J., 2013. Separation of ethylene from refinery dry gas via forming hydrate in w/o dispersion system. Sep. Purif. Technol. 116, 342–350.

Maryam, G., Pakizeh, M., 2017. Development of a new nanofiltration membrane for removal of kinetic hydrate inhibitor from water. Sep. Purif. Technol. 183, 237–248.

Mehta, A.P., Sloan, E.D., 1994. Structure H hydrate phase equilibria of paraffins, naphthenes, and olefins with methane. J. Chem. Eng. Data 39, 887–890.

Ohno, H., Susilo, D.R., Gordienko, R., Ripmeester, J., Walker, V.K., 2010. Interaction of antifreeze proteins with hydrocarbon hydrates. J. Phys. Chem. 16, 10409–10417.

Ohno, H., Moudrakovski, I., Gordienko, R., Ripmeester, J., Walker, V.K., 2012. Structures of hydrocarbon hydrates during formation with and without inhibitors. J. Phys. Chem. 116, 1337–1343.

Parisa, N., Mottahedin, M., Varaminian, F., 2014. Separation of methane–ethane gas mixtures via gas hydrate formation. Sep. Purif. Technol. 123, 139–144.

Peng, B.Z., Chen, J., Sun, C.Y., 2008. Flow characteristics and morphology of hydrate slurry formed from (natural gas + diesel oil/condensate oil+water)system containing anti-agglomerant. Chem. Eng. Sci. 84, 333–344.

Rao, Y.C., Sun, Y., Wang, S.L., Ding, B.Y., 2020. Investigation on gas hydrate formation properties in a spiral flow using a flow loop. Int. J. Oil. Gas. Coal. T. 25, 292–318.

Roosta, H., Khosharay, S., Varaminian, F., 2013. Experimental study of methane hydrate formation kinetics with or without additives and modeling based on chemical affinity. Energ. Convers. Manage. 76, 499–505.

Sanatgar, S.M., Peyvandi, K., 2019. New edible additives as green inhibitors for preventing methane hydrate formation. J. Environ. Chem. Eng. 7, 103172.

Sloan, E.D., 2005. A changing hydrate paradigm-from apprehension to avoidance to risk management. Fluid. Phase. Equilibr. 228, 67–74.

Storr, M.T., Taylor, P.C., Monfort, J.P., Rodger, P.M., 2004. Kinetic inhibitor of hydrate crystallization. J. Am. Chem. Soc. 126, 1569–1576.

Talaghat, B., Reza, M., 2014. Enhancement of the performance of modified starch as a kinetic hydrate inhibitor in the presence of polyoxides for simple gas hydrate formation in a flow mini-loop apparatus. J. Nat. Gas Sci. Eng. 18, 7–12.

Villano, L.D., Kelland, M.A., 2009. Tetrahydrofuran hydrate crystal growth inhibition by hyperbranched poly(ester amide)s. Chem. Eng. Sci. 64, 3197–3200.

Wang, S.L., Huang, J.Y., Yan, S., Rao, Y.C., 2020. Hydrate formation kinetics based on chemical affinity model. Chem. Ind. Eng. Prog. 39, 966–974.

Xi, C.M., Chen, S., Yu, D.M., Wang, S.L., Lv, X.F., Rao, Y.C., 2018. Kinetic study of carbon dioxide hydrate formation in presence of sucrose and attapulgite. Sci. Technol. Eng. 18, 88–94.

Yan, S., Dai, W.J., Wang, S.L., Rao, Y.C., 2018. Graphene oxide: An effective promoter for $CO_2$ hydrate formation. Energies 11, 1756–1769.

York, J.D., Firoozabadi, A., 2008. Alcohol cosurfactants in hydrate antiagglomeration. J. Phys. Chem. B 112, 10455–10465.

Yu, D.M., Chen, S., Wang, S.L., Rao, Y.C., Lv, X.F., 2018. Experiment on attapulgite for $CO_2$ hydrate formation kinetics. Chem. Ind. Eng. Prog. 37, 546–553.

Zeng, H., Wilson, L.D., Walker, V.K., Ripmeester, J.A., 2006. Effect of antifreeze proteins on the nucleation, growth, and the memory effect during tetrahydrofuran clathrate hydrate formation. J. Am. Chem. Soc. 128, 2844–2850.

Zerpa, L.E., Salager, J.L., Koh, C.A., Sloan, E.D., Sum, A.K., 2011. Surface chemistry and gas hydrates in flow assurance. Ind. Eng. Chem. Res. 50, 188–197.

Zhao, H., Sun, M., Firoozabadi, A., 2016. Anti-agglomeration of natural gas hydrates in liquid condensate and crude oil at constant pressure conditions. Fuel 180, 187–193.